

Yukawa Unification in an SO(10) SUSY GUT: SUSY on the Edge

Zijie Poh and Stuart Raby

Department of Physics
The Ohio State University
191 W. Woodruff Ave, Columbus, OH 43210, USA

June 8, 2021

Abstract

In this paper we analyze Yukawa unification in a three family SO(10) SUSY GUT. We perform a global χ^2 analysis and show that SUSY effects do not decouple even though the universal scalar mass parameter at the GUT scale, m_{16} , is found to lie between 15 and 30 TeV with the best fit given for $m_{16} \approx 25$ TeV. Note, SUSY effects don't decouple since stops and bottoms have mass of order 5 TeV, due to RG running from M_{GUT} . The model has many testable predictions. Gauginos are the lightest sparticles and the light Higgs boson is very much Standard Model-like. The model is consistent with flavor and CP observables with the $BR(\mu \rightarrow e\gamma)$ close to the experimental upper bound. With such a large value of m_{16} we clearly cannot be considered “natural” SUSY nor are we “Split” SUSY. We are thus in the region in between or “SUSY on the Edge.”

1 Introduction

Gauge and Yukawa unified SO(10) supersymmetric grand unified theories (SUSY GUTs) [1–5] are a class of highly constrained models. By performing a global fit to low energy data, such as fermion masses and mixing angles and flavor observables, SO(10) SUSY GUT models can provide experimental constraints on sparticle masses accessible at the LHC energy scale. The specific SO(10) SUSY GUT model that we study in this paper has a $D_3 \times [U(1) \times \mathbb{Z}_3 \times \mathbb{Z}_3]$ family symmetry [6, 7]. This model includes three families of quarks and leptons and has been shown to provide good fits to low energy precision electroweak observables, including fermion masses and mixing angles [8–12].

In this paper we extend the analysis of previous papers by including additional low energy flavor observables. We also identify which observables are better fit by incorporating the SUSY effects. We then discuss the many experimental tests of this model. Finally we evaluate the amount of fine-tuning in this scenario. As might be expected the amount of fine-tuning is enormous. However, we show that introducing certain boundary conditions at the GUT scale has the effect of dramatically reducing the amount of fine-tuning. The origin of such boundary conditions in this theoretical sweet spot is not known, although we discuss some possible sources in an Appendix.

The paper is organized as follows. In Section 2, we present an overview of the SO(10) model and `maton`¹, the program that runs all the parameters and calculates most of the observables. In Section 3, we present the results of a global χ^2 analysis for both the universal and “mirage mediated” gaugino mass boundary conditions. We show that χ^2 is minimized for values of the universal scalar mass, m_{16} of order 25 TeV, for both universal gaugino masses at the GUT scale or “mirage mediation” with non-universal gaugino masses, respectively (see Figs. 1 and 3). The χ^2 function now includes the CP-even angular observables of $B^0 \rightarrow K^* \mu^+ \mu^-$ measured by LHCb. Some of these observables are in slight tension with the standard model (SM) prediction [13, 14]. In particular, the observable P'_5 integrated over the dimuon invariant mass squared, $1 \leq q^2 \leq 6 \text{ GeV}^2$, has a 2.5σ discrepancy from the SM prediction. In addition, the angular observable P'_4 integrated over $14.18 \leq q^2 \leq 16 \text{ GeV}^2$ also has a 2.7σ tension with the SM prediction. We also compare our fits to inclusive vs. exclusive measurements of the CKM elements V_{ub} and V_{cb} .

The first two families of squarks and sleptons have mass of order m_{16} and thus they decouple from low energy physics. However, the third family scalars are significantly lighter, with mass between 4 and 10 TeV. This is a consequence of a natural inverted scalar mass hierarchy [15]. Hence they do not decouple and thus contribute to lowering χ^2 . In Section 3.2 we discuss the observables which are better fit by including SUSY loops. We then discuss bounds on the gluino mass in Section 3.3 and further predictions in Section 3.4.

Since our scalar masses are heavy there is, in general, considerable fine-tuning of order 1 part in 10^5 . In Section 4, we present the results of a fine tuning analysis of the model and demonstrate that given particular ratios of soft breaking parameters at the GUT scale the amount of fine tuning is minimized to roughly 1 part in 500 (perhaps these boundaries conditions can be obtained in a fundamental SUSY breaking model). Possible origins for the

¹“maton” was developed by Radovan Dermis ek and modified for large scalar masses by Archana Anandkrishnan, B. Charles Bryant, Zijie Poh and Akin Wingerter.

necessary boundary conditions are discussed in the Appendix.

Finally, we note that our soft breaking parameter m_{16} lies in the range between 15 and 30 TeV. Hence the gravitino mass is expected to be large, perhaps large enough to avoid the cosmological gravitino problem [16]. The moduli may also be suitably heavy to avoid a cosmological moduli problem [17–20]. At the same time we see that SUSY effects have not decoupled from low energy flavor observables, thus our soft SUSY breaking parameters lie on the *edge* between *Split* and *natural* SUSY. We denote this region of parameter space as *SUSY on the Edge*. Gauginos are expected to be visible at the LHC with gluinos decaying predominantly into third generation quarks with special decay signatures. While the light Higgs discovered by CMS and ATLAS is expected to be very much Standard Model-like. We also present predictions for additional flavor and CP violating observables, see Table 4. In Section 5 we conclude and discuss phenomenological tests of our model.

2 Model and Procedure

The details of our SO(10) SUSY GUT model is presented in [9]. The GUT scale boundary conditions that we use are universal squark and slepton masses, m_{16} , universal trilinear couplings, A_0 , and non-universal Higgs masses, m_{H_u} and m_{H_d} . As for the boundary condition for the gaugino masses, we consider two different cases. One with universal gaugino masses, $M_{1/2}$, and another with mirage mediated gaugino masses. The mirage mediated gaugino masses are defined as [10]

$$M_i = \left(1 + \frac{g_G^2 b_i \alpha}{16\pi^2} \log \frac{M_{\text{pl}}}{m_{16}} \right) M_{1/2}, \quad (1)$$

where $M_{1/2}$ and α are free parameters and $b_i = (33/5, 1, -3)$ for $i = 1, 2, 3$ are the appropriate β -function coefficients. Mirage boundary condition is interesting because $\alpha = 1.5$ is the optimal scenario for a well-tempered dark matter [21]. On the other hand, it has been shown that the LSP of universal boundary condition is predominantly Bino-like [11], which leads to an over-closed universe. However, this problem can be solved by introducing axions with mass lighter than the LSP into the model. Hence, in this paper, we study the cases where the universal boundary condition, $\alpha = 0$, and mirage boundary condition with $\alpha = 1.5$.

On the other hand, the charged-fermion sector of our model has 12 parameters - 11 Yukawa parameters and $\tan \beta$. In comparison, the SM has 13 free parameters. Hence, our model has 1 prediction in the charged fermion sector. Including the neutrino sector, our model has 3 additional free parameters to fit 6 observables - 2 Δm^2 s, 3 real mixing angles and one CP violating phase. Hence, our model has 4 predictions in the fermion sector.

To summarize, all the free parameters of our model are listed in Table 1. With universal gaugino masses boundary condition, our model has 24 free parameters while with mirage mediated gaugino mass boundary conditions the number of free parameters increases to 25.

The detailed procedure of our calculation is presented in [9]. In addition, we want to emphasize that after integrating out the right-handed neutrinos, we use the two-loop Minimal Supersymmetric Standard Model (MSSM) renormalization group equation (RGE) to run down to the weak scale. At the weak scale, we include the one-loop threshold corrections for the Yukawa and the gauge couplings, which was calculated by Pierce et. al. [22]. The

Sector	Universal Gaugino Masses	No.	Mirage Mediated Gaugino Masses	No.
Gauge	$\alpha_G, M_G, \epsilon_3$	3	$\alpha_G, M_G, \epsilon_3$	3
SUSY (GUT scale)	$m_{16}, M_{1/2}, A_0, m_{H_u}, m_{H_d}$	5	$m_{16}, M_{1/2}, A_0, m_{H_u}, m_{H_d}, \alpha$	6
Yukawa Textures	$\epsilon, \epsilon', \lambda, \rho, \sigma, \tilde{\epsilon}, \xi, \phi_\rho, \phi_\sigma, \phi_{\tilde{\epsilon}}, \phi_\xi$	11	$\epsilon, \epsilon', \lambda, \rho, \sigma, \tilde{\epsilon}, \xi, \phi_\rho, \phi_\sigma, \phi_{\tilde{\epsilon}}, \phi_\xi$	11
Neutrino	$M_{R_1}, M_{R_2}, M_{R_3}$	3	$M_{R_1}, M_{R_2}, M_{R_3}$	3
SUSY (EW Scale)	$\tan \beta, \mu$	2	$\tan \beta, \mu$	2
Total		24		25

Table 1: Our model has 24 free parameters for universal gaugino masses boundary conditions. For mirage mediated gaugino masses boundary condition, there is an additional input parameter, α , which determines the amount of splitting of the gaugino masses at GUT scale.

gluino mass, $M_{\tilde{g}}$, and CP odd Higgs mass, M_A , are pole masses. However, we do not include one-loop threshold corrections for the other scalar masses. Instead, we estimated that these corrections are about 10%. Hence, the GUT Scale parameters of our model have an inherent 10% theoretical error. Adding the one-loop threshold correction for the soft scalar masses can be a future project.

In addition to calculating the observables included in [9], we included a low q^2 bin ($1 \leq q^2 \leq 6 \text{ GeV}^2$) and a high q^2 bin ($14.18 \leq q^2 \leq 16 \text{ GeV}^2$) for each of the following 4 CP-even $B \rightarrow K^* \mu \mu$ angular observables: F_L, P_2, P'_4 , and P'_5 . We did not include other CP-even observables because the theoretical uncertainty of those observables are much too big. Hence, they do not constrain our model. These angular observables are calculated by **superiso** version 3.4 [23]. Since **superiso** assumes that all soft parameters are real and only takes the diagonal entries of the trilinear couplings into account, we do not include CP-odd $B \rightarrow K^* \mu \mu$ angular observables in our analysis.

Table 2 includes 45 observables that we include in our global χ^2 analysis. The program that calculates these observables and the theoretical errors that are assigned to each observable are also included in the table. The theoretical uncertainty for the $B \rightarrow K^* \mu \mu$ observables are taken from the **superiso** manual. However, since **superiso** does not take into account the imaginary part of the soft parameters, we assigned an additional 15% theoretical errors to the calculation.

To perform the global χ^2 analysis, we construct a χ^2 function

$$\chi^2 = \sum_i \frac{|x_i^{\text{th}} - x_i^{\text{exp}}|^2}{\sigma_i^2}, \quad (2)$$

where x_i^{th} are the calculated values, x_i^{exp} are the experimentally measured values, and σ_i^2 are the sum of the squares of the experimental and theoretical uncertainties, which are also listed in Table 2. To find the minimum of this χ^2 function, we use the **Minuit** package maintained by CERN [24]. As in most minimization problems, obtaining the true global minimum is not guaranteed. To increase the likelihood of obtaining the true global minimum, we iterate the minimization process with random initial guesses for the free parameters.

To calculate the $\chi^2/\text{d.o.f}$, we assume that the observables are uncorrelated. So, for the universal boundary condition, we have $45 - 24 = 21$ degrees of freedom, while for the mirage

boundary condition, we have $45 - 25 = 20$ degrees of freedom. Given these gross assumptions, one should not take the value of $\chi^2/\text{d.o.f}$ too seriously.

3 Results: Global χ^2 Analysis

Several benchmark points with the results of the global χ^2 analysis are given in Appendix A and a plot of χ^2 as a function of the parameter m_{16} is given in Figure 1 or χ^2 contours in the two dimensional plane of $M_{\tilde{g}}$ vs. m_{16} is given in Figure 3. Let us now discuss some features of the results.

3.1 Inclusive vs. Exclusive $|V_{ub}|$ and $|V_{cb}|$

Due to the discrepancy between the values of $|V_{ub}|$ and $|V_{cb}|$ determined from inclusive and exclusive semi-leptonic decay. We define three different χ^2 functions:

1. $|V_{ub}|$ and $|V_{cb}|$ are taken to be the inclusive values
2. $|V_{ub}|$ and $|V_{cb}|$ are taken to be the exclusive values
3. $|V_{ub}|$ and $|V_{cb}|$ are taken to be the average of inclusive and exclusive values with error bars overlapping with the error bars of both the inclusive and the exclusive measurements

The results of these three analyses are shown in Figure 1. We see that for both the universal boundary condition $\alpha = 0$ and mirage boundary condition with $\alpha = 1.5$, the $\chi^2/\text{d.o.f}$ obtained by fitting to the inclusive values are the biggest. Hence, we predict that the exclusive values of $|V_{ub}|$ and $|V_{cb}|$ are the correct values for both universal and mirage gaugino masses.

Since the χ^2 difference between case (2) and case (3) is small and to be conservative, the analyses of the rest of the paper are done for case (3), where $|V_{ub}|$ and $|V_{cb}|$ are the average of the inclusive and exclusive values.

3.2 SUSY Non-decoupled observables

B physics observables

Some of the measured angular observables of $B \rightarrow K^* \mu^+ \mu^-$ are in tension with the SM prediction. For example, P'_4 in the high q^2 bin ($14.18 \leq q^2 \leq 16 \text{ GeV}^2$) has a 2.7σ discrepancy with the SM prediction, P'_5 in the low q^2 bin ($1 \leq q^2 \leq 6 \text{ GeV}^2$) has a 2.5σ discrepancy with the SM prediction, and P_2 in the low q^2 bin has a 2σ discrepancy with the SM prediction [13, 14, 31]. These observables are defined in [32, 33]. In addition, previous analysis [31, 34] found that the tension in P'_4 of the high q^2 bin cannot be explained by the MSSM. On the other hand, the tension of F_L and P'_5 of the low q^2 bin can be explained by the MSSM by having a negative contribution to the C_7 Wilson coefficient. In the standard model $C_7 \approx -0.32$. The tension in F_L and P'_5 can be further reduced by making C_7 more negative [31, 35].

Observable	Exp. Value	Ref.	Program	Th. Error
M_Z	91.1876 ± 0.0021 GeV	[25]	Input	0.0%
M_W	80.385 ± 0.015 GeV	[25]	maton	0.5%
α_{em}	$1/137.035999074(44)$	[25]	maton	0.5%
G_μ	$1.1663787(6) \times 10^{-5}$ GeV ⁻²	[25]	maton	1%
$\alpha_3(M_Z)$	0.1185 ± 0.0006	[25]	maton	0.5%
M_t	$173.21 \pm 0.51 \pm 0.71$ GeV	[25]	maton	0.5%
$m_b(m_b)$	4.18 ± 0.03 GeV	[25]	maton	0.5%
M_τ	1776.82 ± 0.16 MeV	[25]	maton	0.5%
$m_b - m_c$	3.45 ± 0.05 GeV	[25]	maton	10%
$m_c(m_c)$	1.275 ± 0.025 GeV	[25]	maton	0.5%
$m_s(2 \text{ GeV})$	95 ± 5 MeV	[25]	maton	0.5%
$m_s/m_d(2 \text{ GeV})$	$17 - 22$	[25]	maton	0.5%
Q	$21 - 25$	[25]	maton	5%
M_μ	$105.6583715(35)$ MeV	[25]	maton	0.5%
M_e	$0.510998928(11)$ MeV	[25]	maton	0.5%
$ V_{us} $	0.2253 ± 0.0008	[25]	maton	0.5%
$ V_{cb} $ (Inclusive)	0.0422 ± 0.0007	[25]	maton	0.5%
$ V_{cb} $ (Exclusive)	0.0395 ± 0.0008	[25]	maton	0.5%
$ V_{cb} $ (Both)	0.0408 ± 0.0021	[25]	maton	0.5%
$ V_{ub} $ (Inclusive)	0.00441 ± 0.00024	[25]	maton	0.5%
$ V_{ub} $ (Exclusive)	0.00328 ± 0.00029	[25]	maton	0.5%
$ V_{ub} $ (Both)	0.00385 ± 0.00086	[25]	maton	0.5%
$ V_{td} $	0.00840 ± 0.0006	[25]	maton	0.5%
$ V_{ts} $	0.0400 ± 0.0027	[25]	maton	0.5%
$\sin 2\beta$	0.682 ± 0.019	[25]	maton	0.5%
ϵ_K	$(2.2325 \pm 0.0155) \times 10^{-3}$	[25]	susyflavor[26]	10%
$\Delta m_{B_s}/\Delta m_{B_d}$	35.0345 ± 0.3884	[25]	susyflavor[26]	20%
Δm_{B_d}	$(3.337 \pm 0.033) \times 10^{-10}$ MeV	[25]	susyflavor[26]	20%
Δm_{21}^2	$(7.02 - 8.09) \times 10^{-5}$ eV ² (3 σ range)	[27]	maton	0.5%
Δm_{31}^2	$(2.317 - 2.607) \times 10^{-3}$ eV ² (3 σ range)	[27]	maton	0.5%
$\sin^2 \theta_{12}$	$0.270 - 0.344$ (3 σ range)	[27]	maton	0.5%
$\sin^2 \theta_{23}$	$0.382 - 0.643$ (3 σ range)	[27]	maton	0.5%
$\sin^2 \theta_{13}$	$0.0186 - 0.0250$ (3 σ range)	[27]	maton	0.5%
M_h	125.7 ± 0.4 GeV	[25]	splitsuspect[28]	3 GeV
BR($b \rightarrow s\gamma$)	$(343 \pm 21 \pm 7) \times 10^{-6}$	[29]	superiso[23]	40%
BR($B_s \rightarrow \mu^+\mu^-$)	$(2.8^{+0.7}_{-0.6}) \times 10^{-9}$	[30]	susyflavor[26]	20%
BR($B_d \rightarrow \mu^+\mu^-$)	$(3.9^{+1.4}_{-1.4}) \times 10^{-10}$	[30]	susyflavor[26]	20%
BR($B \rightarrow \tau\nu$)	$(114 \pm 22) \times 10^{-6}$	[29]	susyflavor[26]	50%
BR($B \rightarrow K^*\mu^+\mu^-$) $_{1 \leq q^2 \leq 6 \text{ GeV}^2}$	$0.34 \pm 0.03 \pm 0.04 \pm 0.02^{+0.00}_{-0.03} \times 10^{-7}$	[14]	superiso[23]	105%
BR($B \rightarrow K^*\mu^+\mu^-$) $_{14.18 \leq q^2 \leq 16 \text{ GeV}^2}$	$0.45 \pm 0.06 \pm 0.04 \pm 0.04^{+0.00}_{-0.05} \times 10^{-7}$	[14]	superiso[23]	190%
$q_0^2(\text{AFB}(B \rightarrow K^*\mu^+\mu^-))$	$4.9 \pm 0.9 \text{ GeV}^2$	[14]	superiso[23]	25%
$F_L(B \rightarrow K^*\mu^+\mu^-)_{1 \leq q^2 \leq 6 \text{ GeV}^2}$	$0.65^{+0.08+0.03}_{-0.07-0.03}$	[14]	superiso[23]	45%
$F_L(B \rightarrow K^*\mu^+\mu^-)_{14.18 \leq q^2 \leq 16 \text{ GeV}^2}$	$0.33^{+0.08+0.03}_{-0.07-0.03}$	[14]	superiso[23]	80%
$-2P_2 = A_T^{\text{Re}}(B \rightarrow K^*\mu^+\mu^-)_{1 \leq q^2 \leq 6 \text{ GeV}^2}$	$-0.66^{+0.24+0.04}_{-0.22-0.01}$	[14]	superiso[23]	95%
$-2P_2 = A_T^{\text{Re}}(B \rightarrow K^*\mu^+\mu^-)_{14.18 \leq q^2 \leq 16 \text{ GeV}^2}$	$1.00^{+0.00+0.00}_{-0.05-0.02}$	[14]	superiso[23]	45%
$P_4'(B \rightarrow K^*\mu^+\mu^-)_{1 \leq q^2 \leq 6 \text{ GeV}^2}$	$0.58^{+0.36}_{-0.32} \pm 0.06$	[13]	superiso[23]	30%
$P_4'(B \rightarrow K^*\mu^+\mu^-)_{14.18 \leq q^2 \leq 16 \text{ GeV}^2}$	$-0.18^{+0.70}_{-0.54} \pm 0.08$	[13]	superiso[23]	35%
$P_5'(B \rightarrow K^*\mu^+\mu^-)_{1 \leq q^2 \leq 6 \text{ GeV}^2}$	$0.21^{+0.20}_{-0.21} \pm 0.03$	[13]	superiso[23]	45%
$P_5'(B \rightarrow K^*\mu^+\mu^-)_{14.18 \leq q^2 \leq 16 \text{ GeV}^2}$	$-0.79^{+0.20}_{-0.13} \pm 0.18$	[13]	superiso[23]	60%

Table 2: This table includes 45 observables that we fit. All experimental errors are 1σ unless otherwise indicated. Column 4 shows the software package that gives us the theoretical prediction. M_Z is fit precisely to impose electroweak symmetry breaking. To account for the inconsistencies in the inclusive and exclusive measurements of $|V_{ub}|$ and $|V_{cb}|$, we perform the global χ^2 analysis using the inclusive and exclusive measurements separately. We also perform an additional analysis where the error bars of $|V_{ub}|$ and $|V_{cb}|$ cover both the inclusive and exclusive values. In addition to the theoretical errors indicated in **superiso** manual, we added an additional 15% error to each of the $B \rightarrow K^*\mu^+\mu^-$ observables because **superiso** does not take into account the phases of soft terms.

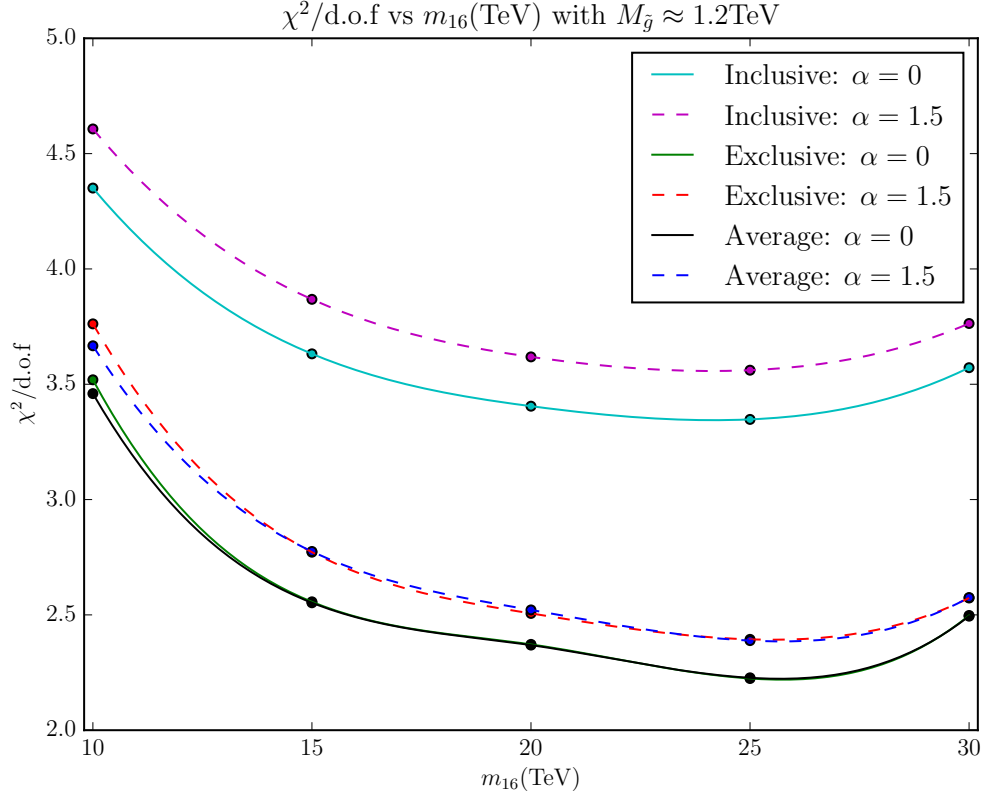


Figure 1: This plot shows the value of $\chi^2/\text{d.o.f}$ as a function of m_{16} for cases where the value of $|V_{ub}|$ and $|V_{cb}|$ are taken to be the inclusive values, the exclusive values, or the average of inclusive and exclusive values. Solid lines refer to the universal boundary condition, $\alpha = 0$, while dashed lines refer to the mirage boundary condition with $\alpha = 1.5$. This plot shows that our model favors the exclusive values of $|V_{ub}|$ and $|V_{cb}|$.

In the MSSM, chargino-stop loops and charged Higgs loop contribute to C_7 . The C_7 contribution from the charged Higgs is always negative. The charged Higgs of our model has mass around 2 TeV. So, the charged Higgs contribution to C_7 is non-negligible and is in the correct direction.

The chargino-stop loop contribution of C_7^{MSSM} has the following form [8]²

$$C_7^{\text{MSSM}} = \frac{\mu A_t \tan \beta}{m_{\tilde{t}}^4} \text{sign}(C_7^{\text{SM}}). \quad (3)$$

Since $\text{sign}(\mu A_t)$ is negative in our model, this term contributes to C_7 in the wrong direction. Hence, to reduce the contribution of this term, our model favors large scalar masses.

From our global χ^2 analysis, we see that the calculated value of P'_4 in the high q^2 bin does not depend on m_{16} , which is expected. In addition, the value of P'_4 calculated in our model is in agreement with the SM. Hence, our results are in agreement with previous analysis that

²Note, the equation for the chargino contribution to C_7^{MSSM} given in Eqn. 21, Ref. [31] apparently has the wrong sign.

the tension in P'_4 cannot be explained in the MSSM. As shown in Table 3, the tension of F_L and P'_5 with the experimental values decreases as m_{16} increases. This is again in agreement with our expectation as explained above.

SUSY corrections to the W mass

On the other hand, the correction for M_W is given by [36–38]

$$\delta M_W \approx \frac{M_W}{2} \frac{c_W^2}{c_W^2 - s_W^2} \Delta\rho \quad (4)$$

and the 1-loop squark contribution is given by

$$\Delta\rho_1^{\text{SUSY}} = \frac{3G\mu}{8\sqrt{2}\pi^2} [-s_t^2 c_t^2 F_0(m_{\tilde{t}_1}^2, m_{\tilde{t}_2}^2) - s_b^2 c_b^2 F_0(m_{\tilde{b}_1}^2, m_{\tilde{b}_2}^2)] \quad (5)$$

$$+ c_t^2 c_b^2 F_0(m_{\tilde{t}_1}^2, m_{\tilde{b}_1}^2) + c_t^2 s_b^2 F_0(m_{\tilde{t}_1}^2, m_{\tilde{b}_2}^2) + s_t^2 c_{\tilde{b}_2} F_0(m_{\tilde{t}_2}^2, m_{\tilde{b}_1}^2) + s_t^2 s_b^2 F_0(m_{\tilde{t}_2}^2, m_{\tilde{b}_2}^2)] \quad (6)$$

where $s_W = \sin \theta_W$, $c_W = \cos \theta_W$, $s_{\tilde{q}} = \sin \theta_{\tilde{q}}$, $c_{\tilde{q}} = \cos \theta_{\tilde{q}}$, and

$$F_0(x, y) = x + y - \frac{2xy}{x - y} \ln \frac{x}{y}. \quad (7)$$

F_0 has properties of $F_0(x, x) = 0$ and $F_0(x, 0) = x$. Hence, we see that when the mass splitting of the squarks is large, the SUSY contribution to the 1-loop M_W can be significant. This is in agreement with our analysis which shows that the pull from M_W increases as the value of m_{16} increases above 20 TeV. Hence, SUSY corrections to M_W are significant and they can go in the right direction.

Light Higgs mass

Fitting to the Higgs mass also constrains the value of m_{16} . The dominant one-loop contribution to the Higgs mass is given by

$$m_h^2 \approx m_Z^2 \cos^2 2\beta + \frac{3}{(4\pi)^2} \frac{m_t^4}{v^2} \left[\ln \frac{M_{\text{SUSY}}^2}{m_t^2} + \frac{X_t}{M_{\text{SUSY}}^2} \left(1 - \frac{X_t^2}{12M_{\text{SUSY}}^2} \right) \right] \quad (8)$$

where $X_t = A_t - \mu/\tan \beta$ is the stop mixing parameter and $M_{\text{SUSY}}^2 = m_{\tilde{t}_1} m_{\tilde{t}_2}$. In our model, $X_t < -\sqrt{6} M_{\text{SUSY}}$ and the ratio X_t/M_{SUSY} becomes less negative as m_{16} increases. Hence, as m_{16} increases, the Higgs mass also increases. The pull in χ^2 due to M_h has a minimum around $m_{16} = 25$ TeV.

Hence, the contributions of M_W , M_h , and b -physics observables to χ^2 , as listed in Table 3, help explain the shape of χ^2 as a function of m_{16} (see Figure 2).

m_{16}	Pull				
	10	15	20	25	30
M_W	0.2110	0.1878	0.1851	0.2320	0.3981
M_h	2.5474	1.1795	0.3454	0.1882	0.6582
$BR(B \rightarrow \tau\nu)$	1.1978	1.3952	1.3557	1.3588	1.3771
$F_L(B \rightarrow K^*\mu^+\mu^-)_{1 \leq q^2 \leq 6 \text{ GeV}^2}$	0.2696	0.2488	0.2219	0.2101	0.2057
$P'_4(B \rightarrow K^*\mu^+\mu^-)_{1 \leq q^2 \leq 6 \text{ GeV}^2}$	1.7066	1.7066	1.7066	1.7066	1.7066
$P'_5(B \rightarrow K^*\mu^+\mu^-)_{1 \leq q^2 \leq 6 \text{ GeV}^2}$	2.4110	2.3432	2.2746	2.2451	2.2339
χ^2	14.1511	8.9744	7.2154	7.0206	7.5220

m_{16}	Fit Value					Exp. Value
	10	15	20	25	30	
M_W	80.4699	80.4606	80.4595	80.4784	80.5454	80.3850
M_h	117.9901	122.1303	124.6547	126.2697	127.6920	125.7000
$BR(B \rightarrow \tau\nu) \times 10^5$	6.6329	6.1340	6.2299	6.2223	6.1778	11.4000
$F_L(B \rightarrow K^*\mu^+\mu^-)_{1 \leq q^2 \leq 6 \text{ GeV}^2}$	0.7434	0.7353	0.7251	0.7207	0.7191	0.6500
$P'_4(B \rightarrow K^*\mu^+\mu^-)_{1 \leq q^2 \leq 6 \text{ GeV}^2}$	0.8174	0.6711	0.5921	0.5717	0.5657	0.5800
$P'_4(B \rightarrow K^*\mu^+\mu^-)_{14.18 \leq q^2 \leq 16 \text{ GeV}^2}$	1.2190	1.2190	1.2190	1.2190	1.2190	-0.1800
$P'_5(B \rightarrow K^*\mu^+\mu^-)_{1 \leq q^2 \leq 6 \text{ GeV}^2}$	-0.7301	-0.5529	-0.4625	-0.4335	-0.4235	0.2100

Table 3: This table shows the set of observables with $\alpha = 0$ and $M_{\tilde{g}} \approx 1.2$ TeV. As argued by Altmannshofer et. al. $B \rightarrow K^*\mu^+\mu^-$ favors large $m_{\tilde{t}}$ [31], which is in agreement with our analysis. On the other hand, as explained in the text, fitting to M_W and M_h disfavors large $m_{\tilde{t}}$. These effects collectively contribute to having a minimum χ^2 around $m_{16} = 25$ TeV. The χ^2 value is plotted as a function of m_{16} in Figure 2. In addition to the observables contributing directly to a minimum of χ^2 at $m_{16} = 25$ TeV, also included in this table is the calculated value of P'_4 at high q^2 bin. This is to illustrate that the value of P'_4 does not depend on the m_{16} , which again agrees with previous analysis [31, 34].

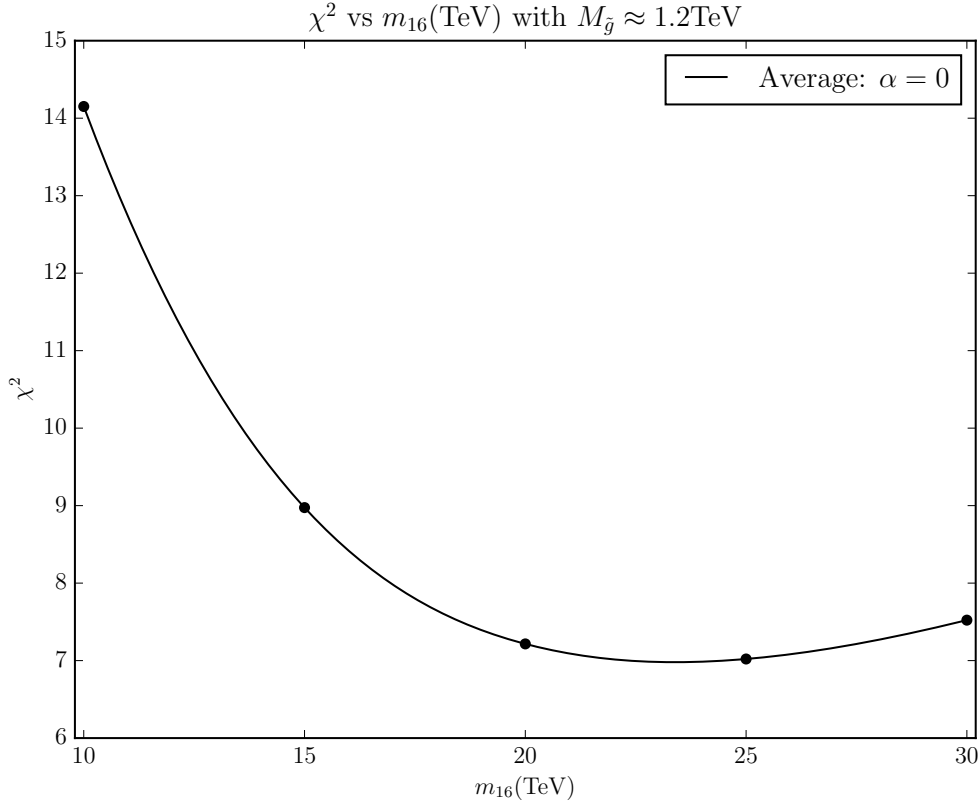


Figure 2: This figure shows the contribution to χ^2 as a function of m_{16} just from the set of observables listed in Table 3. Fitting to the values of M_W , M_h , and b -physics observables listed in Table 3 helps explain why χ^2 is minimized at $m_{16} \approx 25$ TeV.

3.3 Bounds on $M_{\tilde{g}}$

To obtain a better picture for the favored value of gluino mass, we plotted two contour plots of $M_{\tilde{g}}$ vs. m_{16} . One for the universal boundary condition $\alpha = 0$ and another for the mirage boundary condition with $\alpha = 1.5$. The current bound on $M_{\tilde{g}}$, for our model, is around 1.2 TeV [12]. The contour plots are created by calculating $\chi^2/\text{d.o.f}$ for 25 equally distributed values of m_{16} and $M_{1/2}$, which gives us $1 < M_{\tilde{g}} < 2$ TeV. We then use cubic interpolation to obtain the smooth contours of $\chi^2/\text{d.o.f}$.

In addition to the contour lines of the $\chi^2/\text{d.o.f}$, we also plotted a 4σ contour line. From this, we see that for mirage boundary conditions $M_{\tilde{g}} \lesssim 1.8$ TeV. However, for universal boundary condition, the 4σ $M_{\tilde{g}}$ bound can be as high as 3 TeV, which is not shown in the Figure. Hence, for mirage boundary conditions, we expect the 4σ bound on the gluino mass to be within reach in the next run of the LHC. As pointed out by [12], the dominant decay mode of the gluino in the universal gaugino mass boundary condition is $t b \tilde{\chi}_1^\mp$. The remaining decay modes are $t \bar{t} \tilde{\chi}_i^0$ and $b \bar{b} \tilde{\chi}_i^0$ for $i = 1, 2$. On the other hand, the dominant mode for gluino decay in the mirage gaugino mass boundary condition is $t b \tilde{\chi}_i^\mp$ for $i = 1, 2$. In all cases, the dominant signature for gluinos in this model is given by b jets, leptons and missing E_T [12].

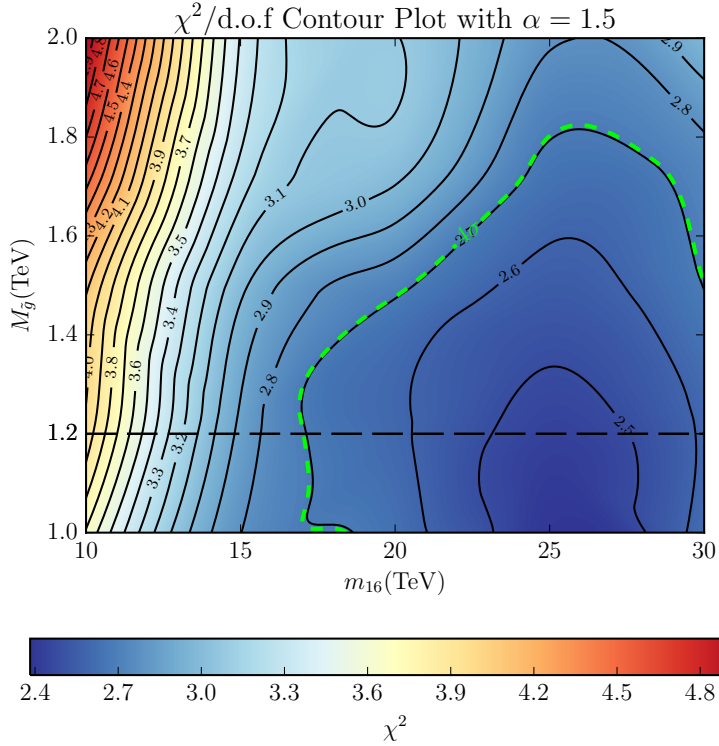
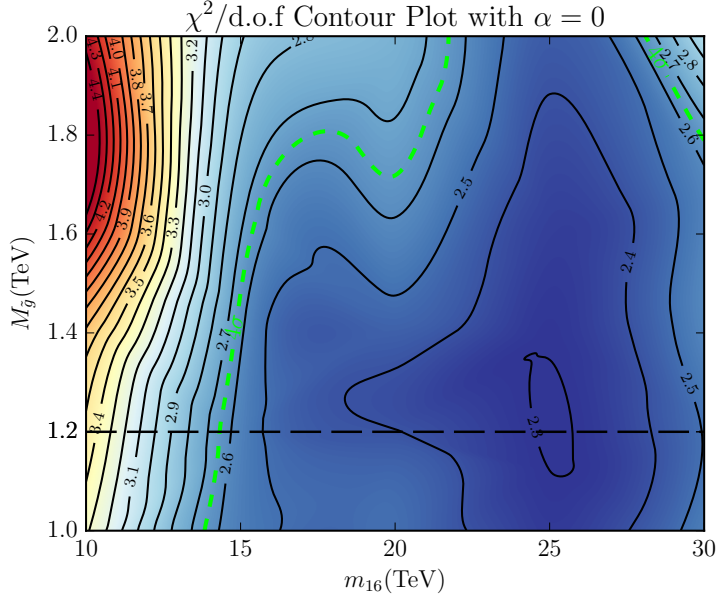


Figure 3: These plots show the contour of $\chi^2/\text{d.o.f}$ as a function of the $M_{\tilde{g}}$ and m_{16} . The 4σ bound is also included in the plot. For $\alpha = 1.5$, the upper bound is within reach of the next run of LHC. In addition, we also see that our model favors $m_{16} \approx 25$ TeV.

3.4 Additional predictions for some benchmark points.

The mass spectrum of the benchmark point of $M_{\tilde{g}} \approx 1.2$ TeV and $m_{16} = 25$ TeV is shown in Table 4. From the χ^2 analysis, we see that the scalar masses are predicted to be around 5 TeV, while the first and second generation scalars have mass around $m_{16} \approx 25$ TeV. With scalars in this mass range, the stop in our model does not completely decouple and can have non-negligible effects on flavor physics. In addition, our light Higgs is SM-like with the heavy Higgs with mass around 2 TeV.

In Table 4, we give the light sparticle masses, the CP violating angle for neutrino oscillations, δ , the branching ratio $BR(\mu \rightarrow e\gamma)$ and the electric dipole moment of the electron for two different values of $M_{\tilde{g}}$ and for $\alpha = 0$ and 1.5. Note that, in general, the gauginos are the lightest sparticles. In addition, $BR(\mu \rightarrow e\gamma)$ and the electric dipole moment of the electron are within reach of future experiments.

m_{16}	25	25	25	25
α	0	1.5	0	1.5
$\chi^2/\text{d.o.f}$	2.158	2.275	2.220	2.505
$m_{\tilde{t}_1}$	4.903	5.011	4.909	5.249
$m_{\tilde{t}_2}$	6.021	6.120	6.033	6.301
$m_{\tilde{b}_1}$	5.989	6.088	6.455	6.606
$m_{\tilde{b}_2}$	6.454	6.541	6.445	6.267
$m_{\tilde{\tau}_1}$	9.880	9.931	9.912	10.040
$m_{\tilde{\tau}_2}$	15.369	15.365	15.393	15.516
$M_{\tilde{g}}$	1.202	1.187	1.613	1.690
$m_{\tilde{\chi}_1^0}$	0.203	0.551	0.279	0.900
$m_{\tilde{\chi}_2^0}$	0.404	0.665	0.538	1.018
$m_{\tilde{\chi}_1^+}$	0.404	0.665	0.538	1.018
$m_{\tilde{\chi}_2^+}$	1.128	1.243	1.232	1.537
M_A	2.194	2.082	2.477	3.352
$\sin \delta$	-0.289	-0.482	-0.520	-0.576
$BR(\mu \rightarrow e\gamma) \times 10^{13}$	1.108	1.430	1.239	1.340
$\text{edm}_e \times 10^{30}(\text{e cm})$	-1.403	-3.305	-1.763	-5.886

Table 4: Predictions with $m_{16} = 25$ TeV for $M_{\tilde{g}} \approx 1.2$ TeV and 1.6 TeV. All masses in the table are in TeV units. Our prediction for the branching ratio $\mu \rightarrow e\gamma$ is consistent with the current upper bound of 5.7×10^{-13} [25]. In addition, our prediction of the electron electric dipole moment is consistent with the current upper bound of 10.5×10^{-28} e cm [25].

4 Results: Fine-Tuning

We studied the fine-tuning of our model using the fine-tuning measure introduced by Ellis et. al. [39], and studied in detail by Barbieri and Giudice [40],

$$\Delta_{\text{BG}} = \max \Delta_{a_i}, \quad \Delta_{a_i} = \left| \frac{\partial \ln M_Z^2}{\partial \ln a_i^2} \right|, \quad (9)$$

where a_i s are input parameters of the model. This fine-tuning measure calculates the sensitivity of M_Z due to a small variation of the input parameters defined at GUT scale.

Electroweak symmetry is broken radiatively in our model. From radiative electroweak symmetry breaking, the CP-odd Higgs mass, m_A , and the μ -term are calculated at one-loop [22]. This calculation requires the physical Z pole mass, M_Z . Hence, in our model, M_Z is fit precisely. To make sure that radiative electroweak symmetry breaking is consistent, m_A and μ are calculated iteratively until they converge.

On the other hand, when we calculate fine-tuning using (9), we use the benchmark points. The benchmark points are the inputs that produce minimum χ^2 value for their respective value of m_{16} and $M_{1/2}$. Hence, at each benchmark point, radiative electroweak symmetry breaking is consistent. Thus, instead of fixing M_Z and calculating m_A and μ iteratively, we then use the value of m_A and μ to calculate M_Z . We then compare this value of M_Z to the exact value to obtain the fine tuning parameter Δ_{BG} .

The input parameters that we vary are $a_i = \{\mu, M_{1/2}, m_{16}, m_{H_u}, m_{H_d}, A_0\}$. The results of our calculations are summarized in Table 5. These results can be understood by the running of GUT scale parameters that contribute to Z mass. For $\tan \beta = 10$, M_Z written in terms of GUT scale parameters is [41–44]

$$M_Z^2 \approx -2.18\mu^2 + 4.22M_{1/2}^2 - 0.82M_{1/2}A_0 + 0.22A_0^2 - 1.27m_{H_u}^2 - 0.053m_{H_d}^2 + 1.34m_{16}^2. \quad (10)$$

Although the above equation is derived for $\tan \beta = 10$, to the lowest order approximation, we do not expect this result to change drastically when $\tan \beta$ increases to ≈ 50 . The calculated fine tuning values shown in Table 5 are of the same order as the fine tuning predicted from this equation. As an example, by direct substitution of the $m_{16} = 20$ TeV benchmark points into the above equation, we find that if $m_{H_{u,d}}/m_{16}$ and A_0/m_{16} are fixed, then $\Delta_{\text{BG}} \approx 2000$ is of the same order as our calculation.

From Table 5, we see that if there are no constraints on the input parameters (first five rows), then the fine-tuning is about 1 part in 10^5 . However, if the GUT scale parameters are constrained such that $m_{H_{u,d}}/m_{16} \approx \sqrt{2}$ and $A_0/m_{16} \approx -2$, then the fine-tuning of our theory is reduced to about 1 part in 500. This suggests that, in a more fundamental natural theory, the ratio of m_{16} with $m_{H_{u,d}}$ and A_0 could be fixed naturally. In the context of the Bear et. al. argument that one should combine dependent terms into a single independent quantity before evaluating fine-tuning[41], we claim that $m_{16}, m_{H_{u,d}}$, and A_0 might be dependent quantities in a more fundamental theory. Hence, one should combine these quantities before calculating fine-tuning. We discuss one possible partial example in the Appendix.

Fine-Tuning of Benchmark Points with $\alpha = 0$ and $M_{\tilde{g}} \approx 1.2$ TeV

Varying Parameters	m_{16}				
	10TeV	15TeV	20TeV	25TeV	30TeV
μ	140	190	210	360	490
$M_{1/2}$	260	340	400	430	450
m_{16}	12000	27000	47000	74000	110000
m_{H_d}	760	1500	3900	6100	8700
m_{H_u}	10000	23000	40000	62000	89000
A_0	9300	21000	39000	61000	85000
m_{16} with A_0/m_{16} fixed	22000	49000	87000	130000	190000
m_{16} with $m_{H_{u,d}}/m_{16}$ fixed	9500	22000	40000	62000	86000
m_{16} with $m_{H_{u,d}}/m_{16}, A_0/m_{16}$ fixed	240	400	630	740	850

 Fine-Tuning of Benchmark Points with $\alpha = 1.5$ and $M_{\tilde{g}} \approx 1.2$ TeV

Varying Parameters	m_{16}				
	10TeV	15TeV	20TeV	25TeV	30TeV
μ	110	240	290	340	380
$M_{1/2}$	320	420	500	560	580
m_{16}	12000	28000	48000	74000	110000
m_{H_d}	750	1500	4600	6000	8500
m_{H_u}	10000	23000	39000	62000	89000
A_0	9200	21000	39000	60000	86000
m_{16} with A_0/m_{16} fixed	22000	49000	87000	130000	190000
m_{16} with $m_{H_{u,d}}/m_{16}$ fixed	9600	21000	39000	61000	87000
m_{16} with $m_{H_{u,d}}/m_{16}, A_0/m_{16}$ fixed	330	450	670	890	1100

Table 5: Without fixing any ratios, the fine-tuning is 1 part in 10^5 . When the ratio of $m_{H_{u,d}}/m_{16}$ and A_0/m_{16} are fixed, the fine-tuning according to (9) is about 1 part in 500. This suggests that these ratios should be fixed in a more fundamental natural theory. In addition, fine-tuning increases as m_{16} increases. Hence, in our model, small m_{16} is favored by naturalness.

5 Conclusion: SUSY on the Edge

We have analyzed a three family SO(10) SUSY GUT with Yukawa unification for the third family. The model gives reasonable fits to fermion masses and mixing angles, as well as many other low energy observables; see Appendix A with some benchmark points of the global χ^2 analysis. A plot of χ^2 as a function of the parameter m_{16} is given in Figure 1 or χ^2 contours in the two dimensional plane of $M_{\tilde{g}}$ vs. m_{16} is given in Figure 3.

We performed an analysis with universal gaugino masses and with non-universal gaugino mass with splitting determined by “mirage mediation” boundary conditions described in Eqn. 1. The parameter $\alpha = 0$ for universal gaugino masses and we also take $\alpha = 1.5$ which is consistent with a well-tempered dark matter candidate [21]. In both cases the model favors $m_{16} \approx 25$ TeV. Nevertheless, due to RG running [15], stops and sbottoms have mass of order 5 TeV, while the first two family scalar masses are of order m_{16} . With m_{16} lying in this mass range, stops in our model do not completely decouple from low energy flavor observables (see Section 3.2). Best fits are found with a gluino mass less than 2 TeV. Our gluinos decay predominantly into third generation quarks [12]. Moreover, in a previous analysis [12] we showed that the dominant LHC signature for gluinos in the model is given by b -Jets, leptons and missing E_T . Note that, in general, the gauginos are the lightest sparticles. The CP odd Higgs mass is of order 2 TeV, thus the light Higg couplings are very much Standard Model-like. In Table 4 we present additional predictions. We give the predictions for the CP violating angle for neutrino oscillations, δ , the branching ratio $BR(\mu \rightarrow e\gamma)$ and the electric dipole moment of the electron for two different values of $M_{\tilde{g}}$ and for $\alpha = 0$ and 1.5. In addition, $BR(\mu \rightarrow e\gamma)$ and the electric dipole moment of the electron are within reach of future experiments. Thus this theory is eminently testable!

We evaluated the amount of high scale fine-tuning of our model. In general we find fine-tuning of order 1 part in 10^5 . However we note that with particular boundary conditions at the GUT scale (when the ratio of m_{16} to A_0 and $m_{H_{u,d}}$ are fixed at $A_0/m_{16} \approx -2$ and $m_{H_{u,d}}/m_{16} \approx \sqrt{2}$) the fine-tuning is reduced to 1 part in 500. We do not have a fundamental theory that gives these two ratios naturally, Nevertheless, in such a fundamental theory the amount of fine-tuning is reduced considerably.

Finally, with the large value of $m_{16} \sim 25$ TeV we expect the gravitino mass to be at least this large. Perhaps it is large enough to avoid a cosmological gravitino problem [16]. In addition, moduli may also be suitably heavy to avoid a cosmological moduli problem [17–20]. Hence the scalar masses are clearly in an intermediate range, i.e. too heavy to be “natural” and lighter than “Split SUSY.” We thus are positioned on the border between these two limiting cases, i.e. this is “SUSY on the **Edge**.”

Acknowledgments

We are indebted to Radovan Dermíšek for his program and his valuable inputs in using it. We are also grateful to B. Charles Bryant and Archana Anandkrishnan for discussions. Z.P. and S.R. received partial support for this work from DOE/ DE-SC0011726. We thank the *Ohio Supercomputer Center* for using their resources.

A Benchmark Points

Table 6: Benchmark point with $m_{16} = 25$ TeV, $M_{\tilde{g}} = 1.202$ TeV, $\alpha = 0$:

$$\begin{aligned}
 (1/\alpha_G, M_G, \epsilon_3) &= (25.98, 2.55 \times 10^{16} \text{ GeV}, -1.30\%) \\
 (\lambda, \lambda\epsilon, \sigma, \lambda\tilde{\epsilon}, \rho, \lambda\epsilon', \lambda\epsilon\xi) &= (0.6101, 0.0308, 1.1559, 0.0049, 0.0698, -0.0019, 0.0036) \\
 (\phi_\sigma, \phi_{\tilde{\epsilon}}, \phi_\rho, \phi_\xi) &= (0.52, 0.58, 3.95, 3.47)\text{rad} \\
 (m_{16}, M_{1/2}, A_0, \mu(M_Z)) &= (25000, 280, -51380, 1212) \text{ GeV} \\
 ((m_{H_d}/m_{16})^2, (m_{H_u}/m_{16})^2, \tan\beta) &= (1.86, 1.61, 50.29) \\
 (M_{R_1}, M_{R_2}, M_{R_3}) &= (9.2, 578.8, 35054.2) \times 10^9 \text{ GeV}
 \end{aligned}$$

Observable	Fit	Exp.	Pull	σ
M_Z	91.1876	91.1876	0.0000	0.4541
M_W	80.4784	80.3850	0.2320	0.4027
$1/\alpha_{\text{em}}$	137.2810	0.0073	0.3569	0.6864
$G_\mu \times 10^5$	1.1789	1.1664	1.0598	0.0118
$\alpha_3(M_Z)$	0.1192	0.1185	0.8199	0.0008
M_t	174.0947	173.2100	0.7171	1.2337
$m_b(m_b)$	4.1986	4.1800	0.5092	0.0366
m_τ	1.7772	1.7768	0.0428	0.0089
$M_b - M_c$	3.1701	3.4500	0.8720	0.3209
$m_c(m_c)$	1.2509	1.2750	0.9333	0.0258
$m_s(2 \text{ GeV})$	0.0953	0.0950	0.0609	0.0050
$m_d/m_s(2 \text{ GeV})$	0.0702	0.0513	2.8247	0.0067
$1/Q^2$	0.0018	0.0019	0.4528	0.0001
M_μ	0.1056	0.1057	0.0578	0.0005
$M_e \times 10^4$	5.1143	5.1100	0.1674	0.0256
$ V_{us} $	0.2245	0.2253	0.5931	0.0014
$ V_{cb} $	0.0404	0.0408	0.1670	0.0021
$ V_{ub} \times 10^3$	3.1235	3.8500	0.8446	0.8601
$ V_{td} \times 10^3$	8.8463	8.4000	0.7418	0.6016
$ V_{ts} $	0.0396	0.0400	0.1508	0.0027
$\sin 2\beta$	0.6296	0.6820	2.7214	0.0193
ϵ_K	0.0022	0.0022	0.0022	0.0002
$\Delta M_{B_s}/\Delta M_{B_d}$	34.8195	35.0345	0.0308	6.9747
$\Delta M_{B_d} \times 10^{13}$	3.9946	3.3370	0.8224	0.7996
$m_{21}^2 \times 10^5$	7.5883	7.5550	0.0621	0.5363
$m_{31}^2 \times 10^3$	2.4649	2.4620	0.0197	0.1455
$\sin^2 \theta_{12}$	0.3028	0.3070	0.1125	0.0370
$\sin^2 \theta_{23}$	0.6600	0.5125	1.1300	0.1305
$\sin^2 \theta_{13}$	0.0162	0.0218	1.7510	0.0032
M_h	126.2697	125.7000	0.1882	3.0265
$BR(B \rightarrow s\gamma) \times 10^4$	2.7220	3.4300	0.5419	1.3064
$BR(B_s \rightarrow \mu^+\mu^-) \times 10^9$	2.7213	2.8000	0.0888	0.8867
$BR(B_d \rightarrow \mu^+\mu^-) \times 10^{10}$	1.0734	3.9000	1.7509	1.6143
$BR(B \rightarrow \tau\nu) \times 10^5$	6.2223	11.4000	1.3588	3.8104
$BR(B \rightarrow K^*\mu^+\mu^-)_{1 \leq q^2 \leq 6 \text{ GeV}^2} \times 10^8$	4.7860	3.4000	0.2739	5.0610
$BR(B \rightarrow K^*\mu^+\mu^-)_{14.18 \leq q^2 \leq 16 \text{ GeV}^2} \times 10^8$	7.5495	5.6000	0.1356	14.3788
$q_0^2(A_{\text{FB}}(B \rightarrow K^*\mu^+\mu^-))$	3.7120	4.9000	0.9190	1.2927
$F_L(B \rightarrow K^*\mu^+\mu^-)_{1 \leq q^2 \leq 6 \text{ GeV}^2}$	0.7207	0.6500	0.2101	0.3366
$F_L(B \rightarrow K^*\mu^+\mu^-)_{14.18 \leq q^2 \leq 16 \text{ GeV}^2}$	0.3108	0.3300	0.0726	0.2644
$P_2(B \rightarrow K^*\mu^+\mu^-)_{1 \leq q^2 \leq 6 \text{ GeV}^2}$	0.0331	0.3300	2.3939	0.1240
$P_2(B \rightarrow K^*\mu^+\mu^-)_{14.18 \leq q^2 \leq 16 \text{ GeV}^2}$	-0.4336	-0.5000	0.3364	0.1974
$P'_4(B \rightarrow K^*\mu^+\mu^-)_{1 \leq q^2 \leq 6 \text{ GeV}^2}$	0.5717	0.5800	0.0208	0.3988
$P'_4(B \rightarrow K^*\mu^+\mu^-)_{14.18 \leq q^2 \leq 16 \text{ GeV}^2}$	1.2190	-0.1800	1.7066	0.8198
$P'_5(B \rightarrow K^*\mu^+\mu^-)_{1 \leq q^2 \leq 6 \text{ GeV}^2}$	-0.4335	0.2100	2.2451	0.2866
$P'_5(B \rightarrow K^*\mu^+\mu^-)_{14.18 \leq q^2 \leq 16 \text{ GeV}^2}$	-0.7116	-0.7900	0.1552	0.5052
Total χ^2			46.7692	

Table 7: Benchmark point with $m_{16} = 25$ TeV, $M_{\tilde{g}} = 1.187$ TeV, $\alpha = 1.5$:

$$\begin{aligned}
 (1/\alpha_G, M_G, \epsilon_3) &= (25.95, 2.60 \times 10^{16} \text{ GeV}, -1.50\%) \\
 (\lambda, \lambda\epsilon, \sigma, \lambda\tilde{\epsilon}, \rho, \lambda\epsilon', \lambda\epsilon\xi) &= (0.6100, 0.0310, 1.1459, 0.0049, 0.0708, -0.0019, 0.0037) \\
 (\phi_\sigma, \phi_{\tilde{\epsilon}}, \phi_\rho, \phi_\xi) &= (0.53, 0.57, 3.94, 3.49)\text{rad} \\
 (m_{16}, M_{1/2}, A_0, \mu(M_Z)) &= (25000, 520, -51157, 1236) \text{ GeV} \\
 ((m_{H_d}/m_{16})^2, (m_{H_u}/m_{16})^2, \tan\beta) &= (1.85, 1.61, 50.19) \\
 (M_{R_1}, M_{R_2}, M_{R_3}) &= (9.1, 567.0, 32370.5) \times 10^9 \text{ GeV}
 \end{aligned}$$

Observable	Fit	Exp.	Pull	σ
M_Z	91.1876	91.1876	0.0000	0.4540
M_W	80.5197	80.3850	0.3344	0.4029
$1/\alpha_{\text{em}}$	137.1416	0.0073	0.1540	0.6857
$G_\mu \times 10^5$	1.1829	1.1664	1.3978	0.0118
$\alpha_3(M_Z)$	0.1189	0.1185	0.4798	0.0008
M_t	173.8449	173.2100	0.5150	1.2328
$m_b(m_b)$	4.2023	4.1800	0.6094	0.0366
m_τ	1.7772	1.7768	0.0450	0.0089
$M_b - M_c$	3.1680	3.4500	0.8791	0.3207
$m_c(m_c)$	1.2570	1.2750	0.6979	0.0258
$m_s(2 \text{ GeV})$	0.0947	0.0950	0.0671	0.0050
$m_d/m_s(2 \text{ GeV})$	0.0700	0.0513	2.7901	0.0067
$1/Q^2$	0.0018	0.0019	0.5027	0.0001
M_μ	0.1056	0.1057	0.1457	0.0005
$M_e \times 10^4$	5.1145	5.1100	0.1775	0.0256
$ V_{us} $	0.2244	0.2253	0.6440	0.0014
$ V_{cb} $	0.0407	0.0408	0.0584	0.0021
$ V_{ub} \times 10^3$	3.1307	3.8500	0.8363	0.8601
$ V_{td} \times 10^3$	8.8596	8.4000	0.7639	0.6016
$ V_{ts} $	0.0398	0.0400	0.0652	0.0027
$\sin 2\beta$	0.6285	0.6820	2.7790	0.0193
ϵ_K	0.0023	0.0022	0.1149	0.0002
$\Delta M_{B_s}/\Delta M_{B_d}$	35.5946	35.0345	0.0786	7.1295
$\Delta M_{B_d} \times 10^{13}$	3.9756	3.3370	0.8025	0.7958
$m_{21}^2 \times 10^5$	7.6111	7.5550	0.1046	0.5364
$m_{31}^2 \times 10^3$	2.4657	2.4620	0.0255	0.1455
$\sin^2 \theta_{12}$	0.3134	0.3070	0.1724	0.0370
$\sin^2 \theta_{23}$	0.6319	0.5125	0.9146	0.1305
$\sin^2 \theta_{13}$	0.0153	0.0218	2.0337	0.0032
M_h	124.5455	125.7000	0.3814	3.0265
$BR(B \rightarrow s\gamma) \times 10^4$	2.7270	3.4300	0.5372	1.3087
$BR(B_s \rightarrow \mu^+\mu^-) \times 10^9$	2.5215	2.8000	0.3228	0.8627
$BR(B_d \rightarrow \mu^+\mu^-) \times 10^{10}$	1.0192	3.9000	1.7861	1.6129
$BR(B \rightarrow \tau\nu) \times 10^5$	6.2272	11.4000	1.3568	3.8124
$BR(B \rightarrow K^*\mu^+\mu^-)_{1 \leq q^2 \leq 6 \text{ GeV}^2} \times 10^8$	4.8580	3.4000	0.2839	5.1361
$BR(B \rightarrow K^*\mu^+\mu^-)_{14.18 \leq q^2 \leq 16 \text{ GeV}^2} \times 10^8$	7.6648	5.6000	0.1415	14.5975
$q_0^2(A_{\text{FB}}(B \rightarrow K^*\mu^+\mu^-))$	3.7150	4.9000	0.9163	1.2933
$F_L(B \rightarrow K^*\mu^+\mu^-)_{1 \leq q^2 \leq 6 \text{ GeV}^2}$	0.7208	0.6500	0.2103	0.3366
$F_L(B \rightarrow K^*\mu^+\mu^-)_{14.18 \leq q^2 \leq 16 \text{ GeV}^2}$	0.3108	0.3300	0.0726	0.2644
$P_2(B \rightarrow K^*\mu^+\mu^-)_{1 \leq q^2 \leq 6 \text{ GeV}^2}$	0.0335	0.3300	2.3879	0.1242
$P_2(B \rightarrow K^*\mu^+\mu^-)_{14.18 \leq q^2 \leq 16 \text{ GeV}^2}$	-0.4336	-0.5000	0.3364	0.1974
$P_4'(B \rightarrow K^*\mu^+\mu^-)_{1 \leq q^2 \leq 6 \text{ GeV}^2}$	0.5697	0.5800	0.0258	0.3985
$P_4'(B \rightarrow K^*\mu^+\mu^-)_{14.18 \leq q^2 \leq 16 \text{ GeV}^2}$	1.2190	-0.1800	1.7066	0.8198
$P_5'(B \rightarrow K^*\mu^+\mu^-)_{1 \leq q^2 \leq 6 \text{ GeV}^2}$	-0.4334	0.2100	2.2450	0.2866
$P_5'(B \rightarrow K^*\mu^+\mu^-)_{14.18 \leq q^2 \leq 16 \text{ GeV}^2}$	-0.7117	-0.7900	0.1550	0.5052
Total χ^2			47.7692	

Table 8: Benchmark point with $m_{16} = 25$ TeV, $M_{\tilde{g}} = 1.613$ TeV, $\alpha = 0$:

$$\begin{aligned}
 (1/\alpha_G, M_G, \epsilon_3) &= (26.22, 2.32 \times 10^{16} \text{ GeV}, -0.65\%) \\
 (\lambda, \lambda\epsilon, \sigma, \lambda\tilde{\epsilon}, \rho, \lambda\epsilon', \lambda\epsilon\xi) &= (0.6096, 0.0311, 1.1398, 0.0049, 0.0710, -0.0019, 0.0038) \\
 (\phi_\sigma, \phi_{\tilde{\epsilon}}, \phi_\rho, \phi_\xi) &= (0.53, 0.56, 3.95, 3.49)\text{rad} \\
 (m_{16}, M_{1/2}, A_0, \mu(M_Z)) &= (25000, 450, -51341, 1226) \text{ GeV} \\
 ((m_{H_d}/m_{16})^2, (m_{H_u}/m_{16})^2, \tan\beta) &= (1.86, 1.61, 50.30) \\
 (M_{R_1}, M_{R_2}, M_{R_3}) &= (9.1, 572.4, 32277.4) \times 10^9 \text{ GeV}
 \end{aligned}$$

Observable	Fit	Exp.	Pull	σ
M_Z	91.1876	91.1876	0.0000	0.4535
M_W	80.4507	80.3850	0.1633	0.4025
$1/\alpha_{\text{em}}$	137.7125	0.0073	0.9825	0.6886
$G_\mu \times 10^5$	1.1732	1.1664	0.5798	0.0117
$\alpha_3(M_Z)$	0.1188	0.1185	0.4140	0.0008
M_t	174.1882	173.2100	0.7927	1.2340
$m_b(m_b)$	4.1954	4.1800	0.4220	0.0366
m_τ	1.7781	1.7768	0.1417	0.0089
$M_b - M_c$	3.1568	3.4500	0.9175	0.3196
$m_c(m_c)$	1.2595	1.2750	0.5993	0.0258
$m_s(2 \text{ GeV})$	0.0939	0.0950	0.2147	0.0050
$m_d/m_s(2 \text{ GeV})$	0.0701	0.0513	2.8052	0.0067
$1/Q^2$	0.0018	0.0019	0.5139	0.0001
M_μ	0.1056	0.1057	0.1818	0.0005
$M_e \times 10^4$	5.1145	5.1100	0.1749	0.0256
$ V_{us} $	0.2244	0.2253	0.6763	0.0014
$ V_{cb} $	0.0404	0.0408	0.1729	0.0021
$ V_{ub} \times 10^3$	3.1033	3.8500	0.8681	0.8601
$ V_{td} \times 10^3$	8.8101	8.4000	0.6817	0.6016
$ V_{ts} $	0.0396	0.0400	0.1531	0.0027
$\sin 2\beta$	0.6270	0.6820	2.8562	0.0193
ϵ_K	0.0022	0.0022	0.2052	0.0002
$\Delta M_{B_s}/\Delta M_{B_d}$	35.3739	35.0345	0.0479	7.0854
$\Delta M_{B_d} \times 10^{13}$	3.9433	3.3370	0.7681	0.7894
$m_{21}^2 \times 10^5$	7.6562	7.5550	0.1886	0.5364
$m_{31}^2 \times 10^3$	2.4631	2.4620	0.0077	0.1455
$\sin^2 \theta_{12}$	0.3170	0.3070	0.2689	0.0370
$\sin^2 \theta_{23}$	0.6264	0.5125	0.8722	0.1305
$\sin^2 \theta_{13}$	0.0149	0.0218	2.1658	0.0032
M_h	124.5054	125.7000	0.3947	3.0265
$BR(B \rightarrow s\gamma) \times 10^4$	2.6840	3.4300	0.5789	1.2887
$BR(B_s \rightarrow \mu^+\mu^-) \times 10^9$	3.0247	2.8000	0.2429	0.9252
$BR(B_d \rightarrow \mu^+\mu^-) \times 10^{10}$	1.1022	3.9000	1.7323	1.6151
$BR(B \rightarrow \tau\nu) \times 10^5$	6.1884	11.4000	1.3727	3.7966
$BR(B \rightarrow K^*\mu^+\mu^-)_{1 \leq q^2 \leq 6 \text{ GeV}^2} \times 10^8$	4.7640	3.4000	0.2707	5.0381
$BR(B \rightarrow K^*\mu^+\mu^-)_{14.18 \leq q^2 \leq 16 \text{ GeV}^2} \times 10^8$	7.5110	5.6000	0.1336	14.3059
$q_0^2(A_{\text{FB}}(B \rightarrow K^*\mu^+\mu^-))$	3.6690	4.9000	0.9579	1.2850
$F_L(B \rightarrow K^*\mu^+\mu^-)_{1 \leq q^2 \leq 6 \text{ GeV}^2}$	0.7225	0.6500	0.2149	0.3374
$F_L(B \rightarrow K^*\mu^+\mu^-)_{14.18 \leq q^2 \leq 16 \text{ GeV}^2}$	0.3108	0.3300	0.0726	0.2644
$P_2(B \rightarrow K^*\mu^+\mu^-)_{1 \leq q^2 \leq 6 \text{ GeV}^2}$	0.0228	0.3300	2.5196	0.1219
$P_2(B \rightarrow K^*\mu^+\mu^-)_{14.18 \leq q^2 \leq 16 \text{ GeV}^2}$	-0.4336	-0.5000	0.3364	0.1974
$P'_4(B \rightarrow K^*\mu^+\mu^-)_{1 \leq q^2 \leq 6 \text{ GeV}^2}$	0.5820	0.5800	0.0050	0.4001
$P'_4(B \rightarrow K^*\mu^+\mu^-)_{14.18 \leq q^2 \leq 16 \text{ GeV}^2}$	1.2190	-0.1800	1.7066	0.8198
$P'_5(B \rightarrow K^*\mu^+\mu^-)_{1 \leq q^2 \leq 6 \text{ GeV}^2}$	-0.4455	0.2100	2.2578	0.2903
$P'_5(B \rightarrow K^*\mu^+\mu^-)_{14.18 \leq q^2 \leq 16 \text{ GeV}^2}$	-0.7116	-0.7900	0.1552	0.5052
Total χ^2			48.8413	

Table 9: Benchmark point with $m_{16} = 25$ TeV, $M_{\tilde{g}} = 1.690$ TeV, $\alpha = 1.5$:

$$\begin{aligned}
 (1/\alpha_G, M_G, \epsilon_3) &= (26.38, 2.09 \times 10^{16} \text{ GeV}, 0.02\%) \\
 (\lambda, \lambda\epsilon, \sigma, \lambda\tilde{\epsilon}, \rho, \lambda\epsilon', \lambda\epsilon\xi) &= (0.6096, 0.0311, 1.1384, 0.0049, 0.0708, -0.0019, 0.0037) \\
 (\phi_\sigma, \phi_{\tilde{\epsilon}}, \phi_\rho, \phi_\xi) &= (0.52, 0.56, 3.96, 3.49)\text{rad} \\
 (m_{16}, M_{1/2}, A_0, \mu(M_Z)) &= (25000, 900, -50846, 1529) \text{ GeV} \\
 ((m_{H_d}/m_{16})^2, (m_{H_u}/m_{16})^2, \tan\beta) &= (1.86, 1.60, 50.31) \\
 (M_{R_1}, M_{R_2}, M_{R_3}) &= (9.1, 579.0, 32367.3) \times 10^9 \text{ GeV}
 \end{aligned}$$

Observable	Fit	Exp.	Pull	σ
M_Z	91.1876	91.1876	0.0000	0.4540
M_W	80.4655	80.3850	0.2000	0.4026
$1/\alpha_{\text{em}}$	137.7323	0.0073	1.0111	0.6887
$G_\mu \times 10^5$	1.1740	1.1664	0.6469	0.0117
$\alpha_3(M_Z)$	0.1188	0.1185	0.2979	0.0008
M_t	174.3427	173.2100	0.9175	1.2345
$m_b(m_b)$	4.2001	4.1800	0.5479	0.0366
m_τ	1.7774	1.7768	0.0644	0.0089
$M_b - M_c$	3.1659	3.4500	0.8863	0.3205
$m_c(m_c)$	1.2574	1.2750	0.6825	0.0258
$m_s(2 \text{ GeV})$	0.0936	0.0950	0.2741	0.0050
$m_d/m_s(2 \text{ GeV})$	0.0701	0.0513	2.8082	0.0067
$1/Q^2$	0.0018	0.0019	0.5170	0.0001
M_μ	0.1056	0.1057	0.1571	0.0005
$M_e \times 10^4$	5.1139	5.1100	0.1545	0.0256
$ V_{us} $	0.2244	0.2253	0.6688	0.0014
$ V_{cb} $	0.0400	0.0408	0.3609	0.0021
$ V_{ub} \times 10^3$	3.0662	3.8500	0.9113	0.8601
$ V_{td} \times 10^3$	8.7156	8.4000	0.5247	0.6016
$ V_{ts} $	0.0392	0.0400	0.2960	0.0027
$\sin 2\beta$	0.6259	0.6820	2.9122	0.0193
ϵ_K	0.0022	0.0022	0.0834	0.0002
$\Delta M_{B_s}/\Delta M_{B_d}$	34.7964	35.0345	0.0342	6.9701
$\Delta M_{B_d} \times 10^{13}$	3.8958	3.3370	0.7165	0.7799
$m_{21}^2 \times 10^5$	7.6614	7.5550	0.1984	0.5364
$m_{31}^2 \times 10^3$	2.4606	2.4620	0.0094	0.1455
$\sin^2 \theta_{12}$	0.3197	0.3070	0.3423	0.0370
$\sin^2 \theta_{23}$	0.6197	0.5125	0.8210	0.1305
$\sin^2 \theta_{13}$	0.0146	0.0218	2.2520	0.0032
M_h	122.0502	125.7000	1.2059	3.0265
$BR(B \rightarrow s\gamma) \times 10^4$	2.6310	3.4300	0.6321	1.2640
$BR(B_s \rightarrow \mu^+\mu^-) \times 10^9$	3.5145	2.8000	0.7203	0.9920
$BR(B_d \rightarrow \mu^+\mu^-) \times 10^{10}$	1.0522	3.9000	1.7647	1.6138
$BR(B \rightarrow \tau\nu) \times 10^5$	6.1009	11.4000	1.4090	3.7610
$BR(B \rightarrow K^*\mu^+\mu^-)_{1 \leq q^2 \leq 6 \text{ GeV}^2} \times 10^8$	4.6780	3.4000	0.2583	4.9484
$BR(B \rightarrow K^*\mu^+\mu^-)_{14.18 \leq q^2 \leq 16 \text{ GeV}^2} \times 10^8$	7.4066	5.6000	0.1281	14.1080
$q_0^2(A_{\text{FB}}(B \rightarrow K^*\mu^+\mu^-))$	3.6290	4.9000	0.9946	1.2779
$F_L(B \rightarrow K^*\mu^+\mu^-)_{1 \leq q^2 \leq 6 \text{ GeV}^2}$	0.7240	0.6500	0.2189	0.3380
$F_L(B \rightarrow K^*\mu^+\mu^-)_{14.18 \leq q^2 \leq 16 \text{ GeV}^2}$	0.3108	0.3300	0.0726	0.2644
$P_2(B \rightarrow K^*\mu^+\mu^-)_{1 \leq q^2 \leq 6 \text{ GeV}^2}$	0.0132	0.3300	2.6254	0.1207
$P_2(B \rightarrow K^*\mu^+\mu^-)_{14.18 \leq q^2 \leq 16 \text{ GeV}^2}$	-0.4337	-0.5000	0.3358	0.1975
$P_4'(B \rightarrow K^*\mu^+\mu^-)_{1 \leq q^2 \leq 6 \text{ GeV}^2}$	0.5918	0.5800	0.0294	0.4014
$P_4'(B \rightarrow K^*\mu^+\mu^-)_{14.18 \leq q^2 \leq 16 \text{ GeV}^2}$	1.2190	-0.1800	1.7066	0.8198
$P_5'(B \rightarrow K^*\mu^+\mu^-)_{1 \leq q^2 \leq 6 \text{ GeV}^2}$	-0.4562	0.2100	2.2685	0.2937
$P_5'(B \rightarrow K^*\mu^+\mu^-)_{14.18 \leq q^2 \leq 16 \text{ GeV}^2}$	-0.7117	-0.7900	0.1550	0.5052
Total χ^2			52.6056	

B Natural SUSY Breaking

Consider Heterotic orbifold models with dilaton/moduli SUSY breaking as discussed in [45]. Following Eqn. (60, 61) in this paper we have the scalar masses for sparticle α , the trilinear couplings and the gaugino masses are given by

$$m_\alpha^2 = m_{3/2}^2(1 + 3C^2 \cos^2 \theta \vec{n}_\alpha \cdot \vec{\Theta}^2) + V_0 \quad (11)$$

$$A_0 = -\sqrt{3}Cm_{3/2}(\sin \theta e^{i\gamma s} + \cos \theta \sum_{i=1}^6 e^{-i\gamma_i} \Theta_i [1 + n_\alpha^{T_i} + n_\beta^{T_i} + n_\gamma^{T_i} - (T_i + T_i^*) \partial_i \log Y_{161016}]), \quad (12)$$

$$M_a = \sqrt{3}m_{3/2} \sin \theta e^{-i\gamma s}, \quad (13)$$

where

$$C^2 = 1 + \frac{V_0}{3m_{10}^2}, \quad (14)$$

V_0 is the tree-level cosmological constant that we will set to be zero, i.e. $C = 1$ and θ determines the amount of SUSY breaking of the dilaton sector versus the moduli sector. $\cos \theta = 0$ means all the SUSY breaking is due to the dilaton. \vec{n}_α are the modular weights of matter fields and $\vec{\Theta}$ gives the probability for the SUSY breaking contribution of each modulus, such that $\sum_{i=1}^6 \Theta_i^2 = 1$. We then let $\theta = 0$ such that at tree level gauginos are massless. They would then obtain one loop suppressed masses due to moduli SUSY breaking. We also assume that the Yukawa couplings, $Y_{\alpha\beta\gamma}$ are independent of the moduli. As a particular example, consider a $\mathbb{Z}_2 \otimes \mathbb{Z}'_6$ orbifold with twist vectors given by $(1/2, 1/2, 0)$, $(1/6, 2/3, 1/6)$ in the three two torii [46]. There are three Kahler moduli in this example. Then we have

$$m_\alpha^2 = m_{3/2}^2(1 + 3(n_\alpha^{T_1} \Theta_1^2 + n_\alpha^{T_3} \Theta_3^2)) \quad (15)$$

where we assumed that $\Theta_2 = 0$.

We now assume that the Higgs 10-plet comes from the bulk on the second two torus. Thus $n_{10}^{T_1} = n_{10}^{T_3} = 0$, $n_{10}^{T_2} = -1$. Hence, $m_{10} = m_{3/2}$ and therefore, $m_{16}^2 = m_{10}^2(1 + 3(n_\alpha^{T_1} \Theta_1^2 + n_\alpha^{T_3} \Theta_3^2))$. If the 16-plet lives in the fifth twisted sector with modular weights, $n_{16}^{T_1} = n_{16}^{T_3} = -1/6$, $n_{16}^{T_2} = -2/3$, we have $m_{16}^2 = \frac{1}{2}m_{10}^2$ or $m_{10} = \sqrt{2}m_{16}$. This is our first constraint, that $m_{10} \equiv (m_{H_u} + m_{H_d})/2 \approx \sqrt{2}m_{16}$.

We then have $A_{(16 \ 16 \ 10)} = -\sqrt{6}m_{16}(e^{-i\gamma_1} \Theta_1 [1 + 2n_{16}^{T_1} + n_{10}^{T_1}] + e^{-i\gamma_3} \Theta_3 [1 + 2n_{16}^{T_3} + n_{10}^{T_3}])$ and we need $A_{(16 \ 16 \ 10)} = A_0 = -2m_{16}$ where the last equality is the boundary condition at the sweet spot. This can be solved with $e^{-i\gamma_1} \Theta_1 = \frac{1}{\sqrt{2}}e^{-i\gamma}$, $e^{-i\gamma_3} \Theta_3 = \frac{1}{\sqrt{2}}e^{+i\gamma}$ and $\gamma = \pi/6$. Of course, it would require the dynamics of stabilizing moduli and SUSY breaking to fix these particular values of Θ_i .

References

- [1] T. Blazek, R. Dermisek, and S. Raby, “Predictions for Higgs and supersymmetry spectra from SO(10) Yukawa unification with μ greater than 0,” *Phys.Rev.Lett.* **88** (2002) 111804, [hep-ph/0107097](#).
- [2] H. Baer and J. Ferrandis, “Supersymmetric SO(10) GUT models with Yukawa unification and a positive μ term,” *Phys.Rev.Lett.* **87** (2001) 211803, [hep-ph/0106352](#).
- [3] T. Blazek, R. Dermisek, and S. Raby, “Yukawa unification in SO(10),” *Phys.Rev.* **D65** (2002) 115004, [hep-ph/0201081](#).
- [4] K. Tobe and J. D. Wells, “Revisiting top bottom tau Yukawa unification in supersymmetric grand unified theories,” *Nucl.Phys.* **B663** (2003) 123–140, [hep-ph/0301015](#).
- [5] D. Auto, H. Baer, C. Balazs, A. Belyaev, J. Ferrandis, *et al.*, “Yukawa coupling unification in supersymmetric models,” *JHEP* **0306** (2003) 023, [hep-ph/0302155](#).
- [6] R. Dermisek and S. Raby, “Bi-large neutrino mixing and CP violation in an SO(10) SUSY GUT for fermion masses,” *Phys.Lett.* **B622** (2005) 327–338, [hep-ph/0507045](#).
- [7] R. Dermisek, M. Harada, and S. Raby, “SO(10) SUSY GUT for Fermion Masses: Lepton Flavor and CP Violation,” *Phys.Rev.* **D74** (2006) 035011, [hep-ph/0606055](#).
- [8] M. Albrecht, W. Altmannshofer, A. J. Buras, D. Guadagnoli, and D. M. Straub, “Challenging SO(10) SUSY GUTs with family symmetries through FCNC processes,” *JHEP* **0710** (2007) 055, [0707.3954](#).
- [9] A. Anandakrishnan, S. Raby, and A. Wingerter, “Yukawa Unification Predictions for the LHC,” *Phys.Rev.* **D87** (2013), no. 5, 055005, [1212.0542](#).
- [10] A. Anandakrishnan and S. Raby, “Yukawa Unification Predictions with effective “Mirage” Mediation,” *Phys.Rev.Lett.* **111** (2013), no. 21, 211801, [1303.5125](#).
- [11] A. Anandakrishnan, B. C. Bryant, S. Raby, and A. Wingerter, “LHC Phenomenology of SO(10) Models with Yukawa Unification,” *Phys.Rev.* **D88** (2013) 075002, [1307.7723](#).
- [12] A. Anandakrishnan, B. C. Bryant, and S. Raby, “LHC Phenomenology of SO(10) Models with Yukawa Unification II,” *Phys.Rev.* **D90** (2014) 015030, [1404.5628](#).
- [13] **LHCb** Collaboration, R. Aaij *et al.*, “Measurement of Form-Factor-Independent Observables in the Decay $B^0 \rightarrow K^{*0} \mu^+ \mu^-$,” *Phys.Rev.Lett.* **111** (2013), no. 19, 191801, [1308.1707](#).
- [14] **LHCb** Collaboration, R. Aaij *et al.*, “Differential branching fraction and angular analysis of the decay $B^0 \rightarrow K^{*0} \mu^+ \mu^-$,” *JHEP* **1308** (2013) 131, [1304.6325](#).

- [15] J. Bagger, J. L. Feng, and N. Polonsky, “Naturally heavy scalars in supersymmetric grand unified theories,” *Nucl.Phys.* **B563** (1999) 3–20, [hep-ph/9905292](#).
- [16] S. Weinberg, “Cosmological Constraints on the Scale of Supersymmetry Breaking,” *Phys.Rev.Lett.* **48** (1982) 1303.
- [17] G. Coughlan, W. Fischler, E. W. Kolb, S. Raby, and G. G. Ross, “Cosmological Problems for the Polonyi Potential,” *Phys.Lett.* **B131** (1983) 59.
- [18] J. R. Ellis, D. V. Nanopoulos, and M. Quiros, “On the Axion, Dilaton, Polonyi, Gravitino and Shadow Matter Problems in Supergravity and Superstring Models,” *Phys.Lett.* **B174** (1986) 176.
- [19] T. Banks, D. B. Kaplan, and A. E. Nelson, “Cosmological implications of dynamical supersymmetry breaking,” *Phys.Rev.* **D49** (1994) 779–787, [hep-ph/9308292](#).
- [20] B. de Carlos, J. Casas, F. Quevedo, and E. Roulet, “Model independent properties and cosmological implications of the dilaton and moduli sectors of 4-d strings,” *Phys.Lett.* **B318** (1993) 447–456, [hep-ph/9308325](#).
- [21] A. Anandakrishnan, B. Shakya, and K. Sinha, “Dark matter at the pseudoscalar Higgs resonance in the phenomenological MSSM and SUSY GUTs,” *Phys.Rev.* **D91** (2015), no. 3, 035029, [1410.0356](#).
- [22] D. M. Pierce, J. A. Bagger, K. T. Matchev, and R.-j. Zhang, “Precision corrections in the minimal supersymmetric standard model,” *Nucl.Phys.* **B491** (1997) 3–67, [hep-ph/9606211](#).
- [23] F. Mahmoudi, “SuperIso v2.3: A Program for calculating flavor physics observables in Supersymmetry,” *Comput.Phys.Commun.* **180** (2009) 1579–1613, [0808.3144](#).
- [24] F. James and M. Roos, “Minuit: A System for Function Minimization and Analysis of the Parameter Errors and Correlations,” *Comput.Phys.Commun.* **10** (1975) 343–367.
- [25] **Particle Data Group** Collaboration, K. Olive *et al.*, “Review of Particle Physics,” *Chin.Phys.* **C38** (2014) 090001.
- [26] A. Crivellin, J. Rosiek, P. Chankowski, A. Dedes, S. Jaeger, *et al.*, “SUSY_FLAVOR v2: A Computational tool for FCNC and CP-violating processes in the MSSM,” *Comput.Phys.Commun.* **184** (2013) 1004–1032, [1203.5023](#).
- [27] M. Gonzalez-Garcia, M. Maltoni, and T. Schwetz, “Updated fit to three neutrino mixing: status of leptonic CP violation,” *JHEP* **1411** (2014) 052, [1409.5439](#).
- [28] N. Bernal, A. Djouadi, and P. Slavich, “The MSSM with heavy scalars,” *JHEP* **0707** (2007) 016, [0705.1496](#).
- [29] **Heavy Flavor Averaging Group (HFAG)** Collaboration, Y. Amhis *et al.*, “Averages of b -hadron, c -hadron, and τ -lepton properties as of summer 2014,” [1412.7515](#).

- [30] **CMS, LHCb** Collaboration, V. Khachatryan *et al.*, “Observation of the rare $B_s^0 \rightarrow \mu^+ \mu^-$ decay from the combined analysis of CMS and LHCb data,” 1411.4413.
- [31] W. Altmannshofer and D. M. Straub, “New physics in $B \rightarrow K^* \mu \mu$?,” *Eur.Phys.J.* **C73** (2013) 2646, 1308.1501.
- [32] S. Descotes-Genon, J. Matias, M. Ramon, and J. Virto, “Implications from clean observables for the binned analysis of $B^- \rightarrow K^* \mu^+ \mu^-$ at large recoil,” *JHEP* **1301** (2013) 048, 1207.2753.
- [33] J. Matias, F. Mescia, M. Ramon, and J. Virto, “Complete Anatomy of $\bar{B}_d^- \rightarrow \bar{K}^{*0} (- \rightarrow K \pi) l^+ l^-$ and its angular distribution,” *JHEP* **1204** (2012) 104, 1202.4266.
- [34] S. Descotes-Genon, J. Matias, and J. Virto, “Understanding the $B \rightarrow K^* \mu^+ \mu^-$ Anomaly,” *Phys.Rev.* **D88** (2013) 074002, 1307.5683.
- [35] F. Mahmoudi, S. Neshatpour, and J. Virto, “ $B \rightarrow K^* \mu^+ \mu^-$ optimised observables in the MSSM,” *Eur.Phys.J.* **C74** (2014), no. 6, 2927, 1401.2145.
- [36] A. Djouadi, P. Gambino, S. Heinemeyer, W. Hollik, C. Junger, *et al.*, “Leading QCD corrections to scalar quark contributions to electroweak precision observables,” *Phys.Rev.* **D57** (1998) 4179–4196, hep-ph/9710438.
- [37] S. Heinemeyer, W. Hollik, and G. Weiglein, “Electroweak precision observables in the minimal supersymmetric standard model,” *Phys.Rept.* **425** (2006) 265–368, hep-ph/0412214.
- [38] V. Barger, P. Huang, M. Ishida, and W.-Y. Keung, “Scalar-Top Masses from SUSY Loops with 125 GeV m_h and Precise M_w ,” *Phys.Lett.* **B718** (2013) 1024–1030, 1206.1777.
- [39] J. R. Ellis, K. Enqvist, D. V. Nanopoulos, and F. Zwirner, “Observables in Low-Energy Superstring Models,” *Mod.Phys.Lett.* **A1** (1986) 57.
- [40] R. Barbieri and G. Giudice, “Upper Bounds on Supersymmetric Particle Masses,” *Nucl.Phys.* **B306** (1988) 63.
- [41] H. Baer, V. Barger, D. Mickelson, and M. Padeffke-Kirkland, “SUSY models under siege: LHC constraints and electroweak fine-tuning,” *Phys.Rev.* **D89** (2014), no. 11, 115019, 1404.2277.
- [42] J. L. Feng, “Naturalness and the Status of Supersymmetry,” *Ann.Rev.Nucl.Part.Sci.* **63** (2013) 351–382, 1302.6587.
- [43] S. P. Martin, “Compressed supersymmetry and natural neutralino dark matter from top squark-mediated annihilation to top quarks,” *Phys.Rev.* **D75** (2007) 115005, hep-ph/0703097.

- [44] T. Kobayashi, H. Terao, and A. Tsuchiya, “Fine-tuning in gauge mediated supersymmetry breaking models and induced top Yukawa coupling,” *Phys.Rev.* **D74** (2006) 015002, [hep-ph/0604091](#).
- [45] A. Brignole, L. E. Ibanez, and C. Munoz, “Soft supersymmetry breaking terms from supergravity and superstring models,” *Adv.Ser.Direct.High Energy Phys.* **21** (2010) 244–268, [hep-ph/9707209](#).
- [46] L. E. Ibanez and D. Lust, “Duality anomaly cancellation, minimal string unification and the effective low-energy Lagrangian of 4-D strings,” *Nucl.Phys.* **B382** (1992) 305–364, [hep-th/9202046](#).